

# Contents

<b>1</b>	<b>Introduction</b>	<b>1</b>
<b>2</b>	<b>Density matrix renormalization group method</b>	<b>2</b>
2.1	Abstract . . . . .	2
2.2	Introduction . . . . .	2
2.3	Density matrix renormalization group . . . . .	3
2.3.1	Real-space renormalization group . . . . .	3
2.3.2	Single particle in a box . . . . .	4
2.3.3	Density matrix method . . . . .	5
2.3.4	Infinite-system method . . . . .	7
<b>3</b>	<b>DRMG applied to two-dimensional classical lattice models</b>	<b>9</b>
3.1	Abstract . . . . .	9
3.2	Partition functions of classical lattices . . . . .	9
3.3	Transfer matrices of lattice models . . . . .	10
3.3.1	1D Ising model . . . . .	10
3.3.2	2D Ising model . . . . .	12
3.4	Partition function of the 2D Ising model as a tensor network .	13
3.4.1	Tensor network of the partition function of a system of four spins . . . . .	14
3.4.2	Thermodynamic limit . . . . .	14
3.4.3	The transfer matrix as a tensor network . . . . .	16
3.5	Transfer matrix renormalization group . . . . .	16
3.5.1	The infinite system algorithm for the transfer matrix .	18
3.5.2	Physical interpretation of the reduced density matrix .	19
3.6	Corner transfer matrix renormalization group . . . . .	21
3.6.1	Corner transfer matrices . . . . .	21
3.6.2	Corner transfer matrix as a tensor network . . . . .	22
3.6.3	Corner transfer matrix renormalization group method	22
3.7	Calculation of observable quantities . . . . .	23
3.8	Validity of approximation . . . . .	23
3.9	Equivalence to variational approximation in the space of ma- trix product states. . . . .	25

<b>4</b>	<b>Critical behaviour and finite-size scaling</b>	<b>26</b>
4.1	Introduction . . . . .	26
<b>A</b>	<b>Correspondence of quantum and classical lattice systems</b>	<b>27</b>
<b>B</b>	<b>Introduction to tensor networks</b>	<b>29</b>
B.1	Tensors, or multidimensional arrays . . . . .	29
B.2	Tensor contraction . . . . .	30
B.3	Tensor networks . . . . .	30
B.3.1	Graphical notation . . . . .	31
B.3.2	Reshaping tensors . . . . .	32
B.3.3	Computational complexity of contraction . . . . .	32
	<b>Bibliography</b>	<b>33</b>

# 1

## Introduction

---

We investigate finite-size scaling behaviour in two-dimensional classical systems using the corner transfer matrix renormalization group (CTMRG) method. Instead of scaling in the system size  $N$ , we perform a scaling analysis in the bond dimension – or numbers of basis states kept – in approximating the corner transfer matrix of the system. This dimension is denoted by  $\chi$  or  $m$ .

This thesis is laid out as follows. Chapter one introduces the density matrix renormalization group (DMRG) method in the context of one-dimensional quantum systems. Since most of the literature and research focuses on quantum lattice models, it is helpful to keep this picture in mind.

Chapter two explains how the ideas of DMRG can be applied to two-dimensional classical lattices. After making this connection clear, we describe the corner transfer matrix renormalization group method, and apply it to the Ising model.

Chapter three introduces the concepts of critical behaviour and finite-size scaling.

Results are presented in chapter four.

Maybe it's better to start with a chapter on statistical mechanics (introducing transfer matrices, computing quantities, etc), then a chapter on critical behaviour and finite-size scaling, and THEN a chapter that introduces DMRG, TMRG and CTMRG in one go.

# 2

## Density matrix renormalization group method

---

### 2.1 Abstract

The density matrix renormalization group, proposed in 1992 by White [13], is introduced in its historical context. To highlight the ideas that led to this method, we explain the real-space renormalization group, proposed by Wilson [16] in 1975. We then explain how the shortcomings of Wilson's method led to the density matrix renormalization group.

### 2.2 Introduction

Consider the problem of numerically finding the ground state  $|\Psi_0\rangle$  of the  $N$ -site 1-dimensional transverse-field Ising-model, given by

$$H = -J \sum_{i=1}^N \sigma_i^z \sigma_{i+1}^z - h \sum_{i=1}^N \sigma_i^x. \quad (2.1)$$

The underlying Hilbert space of the system is a tensor product of the local Hilbert spaces  $\mathcal{H}_{\text{site}}$ , which are spanned by the states  $\{|\uparrow\rangle, |\downarrow\rangle\}$ . Thus, a general state of the system is a unit vector in a  $2^N$ -dimensional space

$$|\Psi\rangle = \sum_{\sigma_1, \sigma_2, \dots \in \{|\uparrow\rangle, |\downarrow\rangle\}} c_{\sigma_1, \sigma_2, \dots, \sigma_N} |\sigma_1\rangle \otimes |\sigma_2\rangle \otimes \dots \otimes |\sigma_N\rangle. \quad (2.2)$$

For a system with 1000 particles, the dimensionality of the Hilbert space comes in at about  $10^{301}$ , some 220 orders of magnitude larger than the number of atoms in the observable universe. How can we possibly hope to approximate states in this space?

As it turns out, nature is very well described by Hamiltonians that are local – that do not contain interactions between an arbitrary number of bodies. And for these Hamiltonians, only an exponentially small subset of states can be explored in the lifetime of the universe [11]. That is, only exponentially few states are physical. The low-energy states, especially, have special properties that allow them to be very well approximated by a polynomial number of parameters. This explains the existence of algorithms, of which the density matrix normalization group is the most widely celebrated one, that can approximate certain quantum systems to machine precision.

Refer to where this will be made more precise.

## 2.3 Density matrix renormalization group

The density matrix renormalization group (DMRG), introduced in 1992 by White [13], aims to find the best approximation of a many-body quantum state, given that only a fixed amount of basis vectors is kept. This amounts to finding the best truncation

$$\mathcal{H}_N \rightarrow \mathcal{H}_{\text{eff}} \quad (2.3)$$

from the full  $N$ -particle Hilbert space to an effective lower dimensional one. This corresponds to renormalizing the Hamiltonian  $H$ .

Before DMRG, several methods for achieving this truncation were proposed, most notably Wilson’s real-space renormalization group [16]. We will discuss this method first, and highlight its shortcomings, which eventually led to the invention of the density-matrix renormalization group method by White.

### 2.3.1 Real-space renormalization group

Consider again the problem of finding the ground state of a many-body Hamiltonian  $H$ . A natural way of renormalizing  $H$  in real-space is by partitioning the lattice in blocks, and writing  $H$  as

$$H = H_A \otimes \dots \otimes H_A \quad (2.4)$$

where  $H_A$  is the Hamiltonian of a block.

Make figures.

The real-space renormalization procedure now entails finding an effective Hamiltonian  $H'_A$  of the two-block Hamiltonian  $H_{AA} = H_A \otimes H_A$ . In the method introduced by Wilson,  $H'_A$  is formed by keeping the  $m$  lowest lying eigenstates  $|\epsilon_i\rangle$  of  $H_{AA}$ :

$$H'_A = \sum_{i=1}^m \epsilon_i |\epsilon_i\rangle \langle \epsilon_i|. \quad (2.5)$$

This is equivalent to writing

$$H'_A = O H_{AA} O^\dagger, \quad (2.6)$$

with  $O$  an  $m \times 2^L$  matrix, with rows being the  $m$  lowest-lying eigenvectors of  $H_{AA}$ , and  $L$  the number of lattice sites of a block. At the fixed point of this iteration procedure,  $H_A$  represents the Hamiltonian of an infinite chain.

Explain renormalization group idea somewhere.

In choosing this truncation, it is assumed that the low-lying eigenstates of the system in the thermodynamic limit are composed of low-lying eigenstates of smaller blocks.

It turns out that this method gives poor results for many lattice systems. Following an example put forth by White and Noack [15], we establish an intuition why.

### 2.3.2 Single particle in a box

Consider the Hamiltonian

$$H = 2 \sum_i |i\rangle \langle i| - \sum_{\langle i,j \rangle} |i\rangle \langle j|, \quad (2.7)$$

where the second summation is over nearest neighbors  $\langle i, j \rangle$ .  $H$  represents the discretized version of the particle-in-a-box Hamiltonian, so we expect its ground state to be approximately a standing wave with wavelength double the box size. However, the blocking procedure just described tries to build the ground state iteratively from ground states of smaller blocks. No matter the amount of states kept, the final result will always incur large errors.

For this simple model, White and Noack solved the problem by diagonalizing the Hamiltonian of a block with different boundary conditions, and combining the lowest eigenstates of each.

Additionally, they noted that diagonalizing  $p > 2$  blocks, and projecting out  $p - 2$  blocks to arrive at  $H_{AA}$  also gives accurate results, and that this is a generalization of applying multiple boundary conditions.

Figure.

In the limit  $p \rightarrow \infty$  this method becomes exact, since we then find exactly the correct contribution of  $H_{AA}$  to the final ground state. It is a slightly changed version of this last method that is now known as DMRG.

### 2.3.3 Density matrix method

The fundamental idea of the density matrix renormalization group method rests on the fact that if we know the state of the final lattice, we can find the  $m$  most important states for  $H_{AA}$  by diagonalizing the reduced density matrix  $\rho_{AA}$  of the two blocks.

To see this, suppose, for simplicity, that the entire lattice is in a pure state<sup>1</sup>  $|\Psi\rangle = \sum c_{b,e} |b\rangle |e\rangle$ , with  $b = 1, \dots, l$  the states of  $H_{AA}$  and  $e = 1, \dots, N_{\text{env}}$  the environment states. The reduced density matrix is given by

$$\rho_{AA} = \sum_e |\Psi\rangle \langle \Psi| = \sum_{b,b'} c_{b,e} c_{b',e} |b\rangle \langle b'| \quad (2.8)$$

We now wish to find a set of orthonormal states  $|\lambda\rangle \in \mathcal{H}_{AA}$ ,  $\lambda = 1, \dots, m$  with  $m < l$ , such that the quadratic norm

$$\| |\Psi\rangle - |\tilde{\Psi}\rangle \| = 1 - 2 \sum_{\lambda,b,e} a_{\lambda,e} c_{b,e} u_{\lambda,b} + \sum_{\lambda,e} a_{\lambda,e}^2 \quad (2.9)$$

is minimized. Here,

$$|\tilde{\Psi}\rangle = \sum_{\lambda=1}^m \sum_{e=1}^{N_{\text{env}}} a_{\lambda,e} |\lambda\rangle |e\rangle \quad (2.10)$$

is the representation of  $|\Psi\rangle$  given the constraint that we can only use  $m$  states from  $\mathcal{H}_{AA}$ . The  $u_{\lambda,b}$  are given by

$$\lambda = \sum_b u_{\lambda,b} |b\rangle. \quad (2.11)$$

---

<sup>1</sup>For a proof for a mixed state, see [10]

We need to minimize (2.9) with respect to  $a_{\lambda,e}$  and  $u_{\lambda,b}$ . Setting the derivative with respect to  $a_{\lambda,e}$  equal to 0 yields

$$-2 \sum_{\lambda,b,e} c_{b,e} u_{\lambda,b} + 2 \sum_{\lambda,e} a_{\lambda,e} = 0 \quad (2.12)$$

So we see that  $a_{\lambda,e} = \sum_b c_{b,e} u_{\lambda,b}$ , and we are left to minimize

$$1 - \sum_{\lambda,b,b'} u_{\lambda,b} (\rho_{AA})_{b,b'} u_{\lambda,b'} \quad (2.13)$$

with respect to  $u_{\lambda,b}$ . But this is equal to

$$1 - \sum_{\lambda=1}^m \langle \lambda | \rho_{AA} | \lambda \rangle \quad (2.14)$$

and because the eigenvalues of  $\rho_{AA}$  represent probabilities and are thus non-negative, this is clearly minimal when  $|\lambda\rangle$  are the  $m$  eigenvectors of  $\rho_{AA}$  corresponding to the largest eigenvalues. This minimal value is

$$1 - \sum_{\lambda=1}^m w_{\lambda} \quad (2.15)$$

with  $w_{\lambda}$  the eigenvalues of the reduced density matrix.

(2.15) is called the truncation error or residual probability, and quantifies the incurred error when taking a number  $m < l$  states to represent  $\mathcal{H}_{AA}$ .

#### Look ahead to SVD

We have proven that the optimal (in the sense that  $\| |\Psi\rangle - |\tilde{\Psi}\rangle \|$  is minimized<sup>2</sup>) states to keep for a subsystem are the states given by the reduced density matrix, obtained by tracing out the entire lattice in the ground state (or some other target state).

The problem, of course, is that we do not know the state of the entire lattice, since that is exactly what we're trying to approximate.

Instead then, we should try to calculate the reduced density matrix of the system embedded in *some* larger environment, as closely as possible resembling the one in which it should be embedded. The combination of the system block and this environment block is usually called *superblock*.

---

<sup>2</sup>There are several other arguments for why these states are optimal, for example, they minimize the error in expectation values  $\langle A \rangle$  of operators. For an overview, see [12].



Analogous to how White and Noack solved the particle in a box problem, we could calculate the ground state of  $p > 2$  blocks, and trace out all but 2, doubling our block size each iteration. In practice, this doesn't work well for interacting Hamiltonians, since this would involve finding the largest eigenvalue of a  $N_{\text{block}}^p \times N_{\text{block}}^p$  matrix (compare this with the particle in a box Hamiltonian, which only grows linearly in the amount of lattice sites).

The widely adopted algorithm proposed by White [14] for finding the ground state of a system in the thermodynamic limit proceeds as follows.

### 2.3.4 Infinite-system method

Add figures.

Mention boundary conditions somewhere

Instead of using an exponential blocking procedure (doubling or tripling the amount of effective sites in a block at each iteration), the infinite-system method in the DMRG formulation adds a single site before truncating the Hilbert space to have at most  $m$  basis states.

1. Consider a block  $A$  of size  $l$ , with  $l$  small. Suppose, for simplicity, that the number of basis states of the block is already  $m$ . States of this block can be written as

$$|\Psi_A\rangle = \sum_{b=1}^m c_b |b\rangle. \quad (2.16)$$

The Hamiltonian is written as (similarly for other operators):

$$\hat{H}_A = \sum_{b,b'}^m H_{bb'} |b\rangle \langle b|. \quad (2.17)$$

2. Construct an enlarged block with one additional site, denoted by  $A\cdot$ . States are now written

$$|\Psi_{A\cdot}\rangle = \sum_{b,\sigma} c_{b,\sigma} |b\rangle \otimes |\sigma\rangle. \quad (2.18)$$

Here,  $\sigma$  runs over the  $d$  local basis states of  $\mathcal{H}_{\text{site}}$ .

3. Construct a superblock, consisting of the enlarged system block  $A\cdot$  and a reflected environment block  $\cdot A$ , together denoted by  $A \cdot \cdot A$ . Find the ground state  $|\Psi_0\rangle$  of  $A \cdot \cdot A$ , for example with the Lanczos method [7].
4. Obtain the reduced density matrix of the enlarged block by tracing out the environment, and write it in diagonal form.

$$\begin{aligned}\rho_{A\cdot} &= \sum_{e,\sigma} (|\sigma\rangle \otimes |e\rangle) |\Psi_0\rangle \langle\Psi_0| (|\sigma\rangle \otimes |e\rangle), \\ &= \sum_{i=1}^{dm} w_i |\lambda_i\rangle \langle\lambda_i|. \end{aligned} \quad (2.19)$$

Here, we have chosen  $w_0 \geq w_1 \dots \geq w_{dm}$ . In this basis, the Hamiltonian is written as

$$\hat{H}_{A\cdot} = \sum_{i,j}^{dm} H_{ij} |\lambda_i\rangle \langle\lambda_j|. \quad (2.20)$$

5. Truncate the Hilbert space by keeping only the  $m$  eigenstates of  $\rho_{A\cdot}$  with largest eigenvalues. Operators truncate as follows:

$$\tilde{\rho}_{A\cdot} = \sum_{i=1}^m w_i |\lambda_i\rangle \langle\lambda_i|, \quad (2.21)$$

$$\tilde{H}_{A\cdot} = \sum_{i,j}^m H_{ij} |\lambda_i\rangle \langle\lambda_j|. \quad (2.22)$$

6. Set  $H_A \leftarrow \tilde{H}_{A\cdot}$  and return to 1.

Expand. Present or link to some results. Finite-system algorithm. Maybe in other chapter: rephrase in MPS, validity of approximation: primer on entropy and eigenvalue spectrum of density matrix.

This methods finds ground state energies with astounding accuracy, and has been the reference point in all 1D quantum lattice simulation since its invention.

# 3

## DRMG applied to two-dimensional classical lattice models

---

### 3.1 Abstract

This chapter explains how to apply to ideas of the density matrix renormalization group to two-dimensional classical lattices. The Ising model is used throughout.

First, we explain the transfer-matrix formulation for classical partition functions.

Then, we show how to renormalize the transfer matrix using DMRG. This was first done by Nishino [8]. To make notation easier, we redefine the transfer matrix in terms of a tensor network.

Then, we explain the corner transfer matrix renormalization group. This method, first introduced by Nishino and Okunishi [9], combines ideas from Baxter [2, 3, 4] and White [13] to significantly speed up the renormalization of the transfer matrix.

### 3.2 Partition functions of classical lattices

The central quantity in equilibrium statistical mechanics is the partition function  $Z$ , which, for a discrete system such as a lattice, is defined as

$$Z = \sum_s \exp(-\beta H(s)), \quad (3.1)$$

where the sum is over all microstates  $s$ ,  $H$  is the energy function, and  $\beta = T^{-1}$  the inverse temperature.

### 3.3 Transfer matrices of lattice models

Transfer matrices are used to re-express the partition function of classical lattice systems, allowing them to be solved exactly or approximated.

We will introduce the transfer matrix in the context of the 1D classical Ising model, first introduced and solved using the transfer matrix method by Ising [6] in his PhD thesis.

#### 3.3.1 1D Ising model

talk a bit about model (magnetism etc).

Somewhere, I should introduce – very briefly – how the magnetization and free energy per site are defined. Maybe just calculate them for 1D Ising model.

Consider the 1D zero-field ferromagnetic Ising model [6], defined by the energy function

$$H(\sigma) = -J \sum_{\langle ij \rangle} \sigma_i \sigma_j. \quad (3.2)$$

Here, we sum over nearest neighbors  $\langle ij \rangle$  and the spins  $\sigma_i$  take the values  $\pm 1$ .  $J > 0$ .

Assume, for the moment, that the chain consists of  $N$  spins, and apply periodic boundary conditions. The partition function of this system is given by

$$Z_N = \sum_{\sigma_1, \dots, \sigma_N \in \{-1, 1\}} \exp(-\beta H(\sigma)) \quad (3.3)$$

Exploiting the local nature of the interaction between spins, we can write

$$Z_N = \sum_{\sigma_1, \dots, \sigma_N \in \{-1, 1\}} \prod_{\langle i, j \rangle} e^{K \sigma_i \sigma_j} \quad (3.4)$$

where we defined  $K \equiv \beta J$ .

Now, we define the  $2 \times 2$  matrix

$$T_{\sigma\sigma'} = \exp(K\sigma\sigma'). \quad (3.5)$$

A possible choice of basis is

$$(|\uparrow\rangle = 1, |\downarrow\rangle = -1) = \left( \begin{bmatrix} 1 \\ 0 \end{bmatrix}, \begin{bmatrix} 0 \\ 1 \end{bmatrix} \right). \quad (3.6)$$

In terms of this matrix,  $Z_N$  is written as

$$Z_N = \sum_{\sigma_1, \dots, \sigma_N} T_{\sigma_1 \sigma_2} \cdots T_{\sigma_N \sigma_1} = \text{Tr } T^N. \quad (3.7)$$

$T$  is called the transfer matrix. In the basis of Equation 3.6,  $T$  is written as

$$T = \begin{bmatrix} e^K & e^{-K} \\ e^{-K} & e^{-K} \end{bmatrix}. \quad (3.8)$$

$T$  is, in fact, diagonalizable. So, we can write  $T^N = P D^N P^{-1}$ , where  $P$  consists of the eigenvectors of  $T$ , and  $D$  has the corresponding eigenvalues on the diagonal. By the cyclic property of the trace, we have

$$Z_N = \lambda_1^N + \lambda_2^N, \quad (3.9)$$

where

$$\begin{aligned} \lambda_1 &= e^K + e^{-K}, \\ \lambda_2 &= e^K - e^{-K}. \end{aligned}$$

Thus, we have reduced the problem of finding the partition function to an eigenvalue problem.

In the thermodynamic limit  $N \rightarrow \infty$

$$Z = \lim_{N \rightarrow \infty} \lambda_1^N \quad (3.10)$$

where  $\lambda_1$  is the non-degenerate largest eigenvalue (in absolute value) of  $T$ .

### Fixed boundary conditions

We may also apply fixed boundary conditions. The partition function is then written as

$$Z_N = \langle \sigma' | T^N | \sigma \rangle, \quad (3.11)$$

where  $|\sigma\rangle$  and  $|\sigma'\rangle$  are the right and left boundary spins.

In the large- $N$  limit,  $T^N$  tends towards the projector onto the eigenspace spanned by the eigenvector belonging to the largest eigenvalue

$$|\lambda_1\rangle = \lim_{N \rightarrow \infty} \frac{T^N |\sigma\rangle}{\|T^N |\sigma\rangle\|}. \quad (3.12)$$

Equation 3.12 is true for any  $|\sigma\rangle$  that is not orthogonal to  $|\lambda_1\rangle$ .

The physical significance of the normalized lowest-lying eigenvector  $|\lambda_1\rangle$  is that  $\langle\lambda_1|\uparrow\rangle$  and  $\langle\lambda_1|\downarrow\rangle$  represent the Boltzmann weight of  $|\uparrow\rangle$  and  $|\downarrow\rangle$  at the boundary of a half-infinite chain.

Maybe picture of above claim?

### 3.3.2 2D Ising model

Talk about exact solution (Onsager). Why is it important? Maybe star-triangle relation (Baxter). Not all IRF models solvable.

Next, we treat the two-dimensional, square-lattice Ising model. In two dimensions, the energy function is still written as in Equation 3.2, but now every lattice site has four neighbors.

Let  $N$  be the number of columns and  $l$  be the number of rows of the lattice, and assume  $l \gg N$ . In the vertical direction, we apply periodic boundary conditions, as in the one-dimensional case. In the horizontal direction, we keep an open boundary. We refer to  $N$  as the system size.

Picture.

Similarly as in the 1D case, the partition function can be written as

$$Z_N = \sum_{\sigma} \prod_{\langle i,j,k,l \rangle} W(\sigma_i, \sigma_j, \sigma_k, \sigma_l) \quad (3.13)$$

where the product runs over all groups of four spins sharing the same face. The Boltzmann weight of such a face is given by

$$W(\sigma_i, \sigma_j, \sigma_k, \sigma_l) = \exp \left\{ \frac{K}{2} (\sigma_i \sigma_j + \sigma_j \sigma_k + \sigma_k \sigma_l + \sigma_l \sigma_i) \right\} \quad (3.14)$$

We can express the Boltzmann weight of a configuration of the whole lattice as a product of the Boltzmann weights of the rows

$$Z_N = \sum_{\sigma} \prod_{r=1}^l W(\sigma_1^r, \sigma_2^r, \sigma_1^{r+1}, \sigma_2^{r+1}) \dots W(\sigma_{N-1}^r, \sigma_N^r, \sigma_{N-1}^{r+1}, \sigma_N^{r+1}) \quad (3.15)$$

where  $\sigma_i^r$  denotes the value of the  $i$ th spin of row  $r$ .

Now, we can generalize the definition of the transfer matrix to two dimensions, by defining it as the Boltzmann weight of an entire row

$$T_N(\sigma, \sigma') = W(\sigma_1, \sigma_2, \sigma'_1, \sigma'_2) \dots W(\sigma_{N-1}, \sigma_N, \sigma'_{N-1}, \sigma'_N) \quad (3.16)$$

If we take the spin configurations of an entire row as basis vectors,  $T_N$  can be written as a matrix of dimensions  $2^N \times 2^N$ .

Similarly as in the one-dimensional case, the partition function now becomes

$$Z_N = \sum_{\sigma} \prod_{r=1}^l T_N(\sigma^r, \sigma^{r+1}) = \text{Tr} T_N^l \quad (3.17)$$

In the limit of an  $N \times \infty$  cylinder, the partition function is once again determined by the largest eigenvalue<sup>1</sup>.

$$Z_N = \lim_{l \rightarrow \infty} T_N^l = \lim_{l \rightarrow \infty} (\lambda_0)^l_N \quad (3.18)$$

The partition function in the thermodynamic limit is given by

$$Z = \lim_{N \rightarrow \infty} Z_N \quad (3.19)$$

### 3.4 Partition function of the 2D Ising model as a tensor network

In calculating the partition function of 1D and 2D lattices, matrices of Boltzmann weights like  $W$  and  $T$  play a crucial role. We have formulated them in a way that is valid for any interaction-round-a-face (IRF) model, defined by

$$H \sim \sum_{\langle i,j,k,l \rangle} W(\sigma_i, \sigma_j, \sigma_k, \sigma_l), \quad (3.20)$$

where the summation is over all spins sharing a face.  $W$  can contain 4-spin, 3-spin, 2-spin and 1-spin interaction terms. The Ising model is a special case of the IRF model, with  $W$  given by Equation 3.14.

We will now express the partition function of the 2D Ising model as a tensor network. The transfer matrix  $T$  is redefined in the process. This allows us to visualize the equations in a way that is consistent with the many other tensor network algorithms under research today. For an introduction to tensor network notation, see Appendix B.

---

<sup>1</sup>As in the 1D case,  $T$  is symmetric, so it is orthogonally diagonalizable.

### 3.4.1 Tensor network of the partition function of a system of four spins

We define

$$Q(\sigma_i, \sigma_j) = \exp(K\sigma_i\sigma_j) \quad (3.21)$$

as the Boltzmann weight of the bond between  $\sigma_i$  and  $\sigma_j$ . It is the same as the 1D transfer matrix in Equation 3.5.

The Boltzmann weight of a face  $W$  decomposes into a product of Boltzmann weights of bonds

$$W(\sigma_i, \sigma_j, \sigma_k, \sigma_l) = Q(\sigma_i, \sigma_j)Q(\sigma_j, \sigma_l)Q(\sigma_l, \sigma_k)Q(\sigma_k, \sigma_i). \quad (3.22)$$

It is now easy to see that the partition function is equal to the contracted tensor network in Figure 3.1:

$$\begin{aligned} Z_{2 \times 2} &= \sum_{\sigma_1, \sigma_2, \sigma_3, \sigma_4} \sum_{a, b, c, d} \delta_{\sigma_1, a} Q(a, b) \delta_{\sigma_2, b} Q(b, c) \delta_{\sigma_3, c} Q(c, d) \delta_{\sigma_4, d} Q(d, a) \\ &= \sum_{\sigma_1, \sigma_2, \sigma_3, \sigma_4} W(\sigma_1, \sigma_2, \sigma_3, \sigma_4). \end{aligned} \quad (3.23)$$

where the Kronecker delta is defined as usual:

$$\delta_{ij} = \begin{cases} 1 & \text{if } i = j \\ 0 & \text{if } i \neq j. \end{cases} \quad (3.24)$$

### 3.4.2 Thermodynamic limit

We define the matrix  $P$  by

$$P^2 = Q. \quad (3.25)$$

as in Figure 3.2. This allows us to write the partition function of an arbitrary  $N \times l$  square lattice as a tensor network of a single recurrent tensor  $a_{ijkl}$ , given by

$$a_{ijkl} = \sum_{a, b, c, d} \delta_{abcd} P_{ia} P_{jb} P_{kc} P_{ld}, \quad (3.26)$$



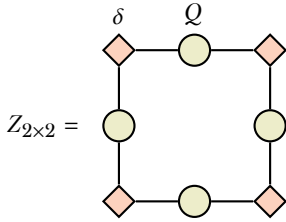


Figure 3.1: A tensor network representation of the partition function of the Ising model on a  $2 \times 2$  lattice. See Equation 3.23.

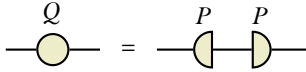


Figure 3.2: Graphical form of Equation 3.25.

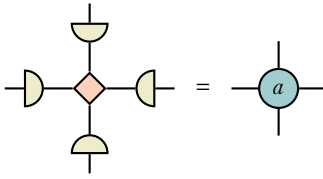


Figure 3.3: Graphical form of Equation 3.26.

where the generalization of the Kronecker delta is defined as

$$\delta_{i_1 \dots i_n} = \begin{cases} 1 & \text{if } i_1 = \dots = i_n \\ 0 & \text{otherwise.} \end{cases} \quad (3.27)$$

See Figure 3.3 and Figure 3.4. At the edges and corners, we define suitable tensors of rank 3 and 2, which we will also denote by  $a$ :

$$\begin{aligned} a_{ijk} &= \sum_{abc} \delta_{abc} P_{ia} P_{jb} P_{kc}, \\ a_{ij} &= \sum_{ab} \delta_{ab} P_{ia} P_{jb}. \end{aligned}$$

The challenge is to approximate this tensor network in the thermodynamic limit.

### 3.4.3 The transfer matrix as a tensor network

Say something about reshaping legs. It is implicit now.

With our newfound representation of the partition function as a tensor network, we can redefine the row-to-row transfer matrix from Equation 3.16 as the tensor network expressed in Figure 3.5. For all  $l$ , it is still true that

$$Z_{N \times l} = \text{Tr} T_N^l = \sum_{i=1}^{2^N} \lambda_i^l, \quad (3.28)$$

so the eigenvalues must be the same. That means that the new definition of the transfer matrix is related to the old one by a basis transformation

$$T_{\text{new}} = P T_{\text{old}} P^T. \quad (3.29)$$

## 3.5 Transfer matrix renormalization group

There is a deep connection between quantum mechanical lattice systems in  $d$  dimensions and classical lattice systems in  $d+1$  dimensions. Via the imaginary time path integral formulation, the partition function of a one-dimensional

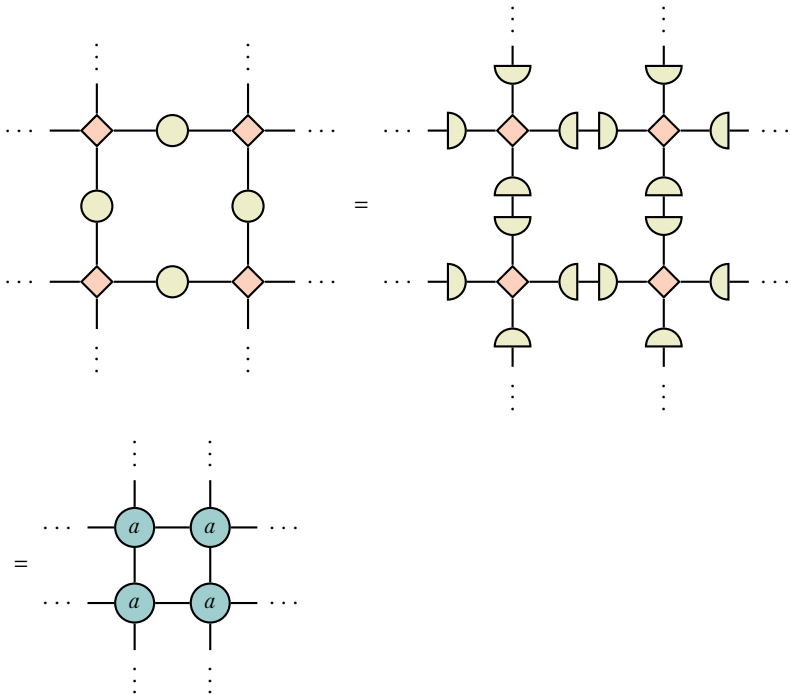


Figure 3.4:  $Z_{N \times l}$  can be written as a contracted tensor network of  $N \times l$  copies of the tensor  $a$ .

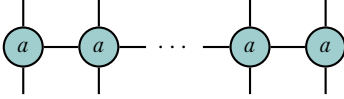


Figure 3.5: The definition of  $T_N$  as a network of  $N$  copies of the tensor  $a$ .

quantum system can be written as the partition function of an effective two-dimensional classical system. The ground state of the quantum system corresponds to the largest eigenvector of the transfer matrix of the classical system.

For more on the quantum-classical correspondence, see Appendix A.

### 3.5.1 The infinite system algorithm for the transfer matrix

Nishino [8, 9] was the first to apply density matrix renormalization group methods in the context of two-dimensional classical lattices.

Analogous to the infinite system DMRG algorithm for approximating the Hamiltonian of quantum spin chains, our goal is to approximate the transfer matrix in the thermodynamic limit as well as possible within a restricted number of basis states  $m$ . We will do this by adding a single site at a time, and truncating the dimension from  $2m$  to  $m$  at each iteration.

For simplicity, we assume that, at the start of the algorithm, the transfer matrix already has dimension  $m$ . We call this transfer matrix  $P_N$ . A good choice of initial transfer matrix is obtained by contracting a couple of  $a$ -tensors, until dimension  $m$  is reached. See Figure 3.6.

To specify fixed instead of open boundary conditions, we may use as boundary tensor a slightly modified version of the three-legged version of  $a$ , namely

$$a_{ijk}^\sigma = \sum_{abc} \delta_{\sigma abc} P_{ia} P_{jb} P_{kc}, \quad (3.30)$$

that represents an edge site with spin fixed at  $\sigma$ .

We enlarge the system with one site by contracting with an additional  $a$ -tensor, obtaining  $P_{N+1}$ . See the first network in Figure 3.7.

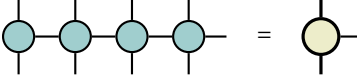


Figure 3.6: A good starting point for the half-row transfer  $P_N$  is obtained by contracting a couple of  $a$ -tensors, until  $P_N$  reaches dimension  $m$ .

In order to find the best projection from  $2m$  basis states back to  $m$ , we embed the system in an environment that is the mirror image of the system we presently have. We call this matrix  $T_{2N+2}$ . It represents the transfer matrix of  $2N+2$  sites. We find the largest eigenvalue and corresponding eigenvector, as shown in Figure 3.8.

The equivalent of the *reduced density matrix of a block* in the classical case is:

$$\rho_{N+1} = \sum_{\sigma_B} \langle \sigma_B | \lambda_0 \rangle \langle \lambda_0 | \sigma_B \rangle, \quad (3.31)$$

where we have summed over all the degrees of freedom of one of the half-row transfer matrices  $P_{N+1}$ . See the first step of Figure 3.9.

The optimal renormalization

$$\tilde{P}_{N+1} = O P_{N+1} O^\dagger \quad (3.32)$$

is obtained by diagonalizing  $\rho_{N+1}$  and keeping the eigenvectors corresponding to the  $m$  largest eigenvalues. See the second step of Figure 3.9.

With this blocking procedure, we can successively find

$$P_{N+1} \rightarrow P_{N+2} \rightarrow \dots, \quad (3.33)$$

until we have reached some termination condition.

Say something about termination condition.

### 3.5.2 Physical interpretation of the reduced density matrix

Generalizing the remarks from section 3.3.1 to the two-dimensional case, we see that the normalized lowest-lying eigenvector of the transfer matrix  $T_N$  contains the Boltzmann weights of spin configurations on the boundary of a half-infinite  $N \times \infty$  lattice.

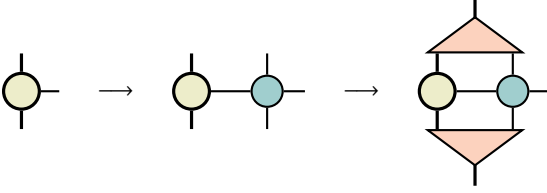


Figure 3.7: In the first step,  $P_{N+1}$  is obtained by contracting the current half-row transfer matrix  $P_N$  with an additional  $a$ -tensor. In the second step,  $P_{N+1}$  is truncated back to an  $m$ -dimensional matrix, with the optimal low-rank approximation given by keeping the basis states corresponding to the  $m$  largest eigenvalues of the density matrix. See Figure 3.9.

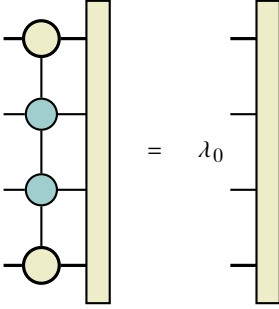


Figure 3.8: Equation for the lowest-lying eigenvector of the row-to-row transfer matrix  $T_{2N+2}$ .

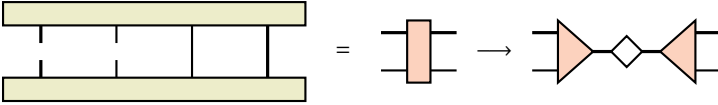


Figure 3.9: Graphical form of Equation 3.31. In the second step,  $\rho_{N+1}$  is diagonalized and only the eigenvectors corresponding to the  $m$  largest eigenvalues are kept.

Therefore, the classical equivalent of the quantum mechanical reduced density matrix, given by Equation 3.31, and by the first network in Figure 3.9, represents the Boltzmann weights of configurations along a cut in an  $N \times \infty$  lattice.

Nishino and Okunishi [9], drawing on ideas from Baxter, realized the Boltzmann weights of configurations along this cut could be obtained by employing *corner transfer matrices*, making it unnecessary to solve the eigenvalue problem in Figure 3.8. Their method, called the Corner Transfer Matrix Renormalization Group method, consumes far less resources while maintaining precision. For this reason, it is the method of choice for most of the simulations in this thesis.

## 3.6 Corner transfer matrix renormalization group

### 3.6.1 Corner transfer matrices

The concept of corner transfer matrices for 2D lattices was first introduced by Baxter [2, 3, 4]. Whereas the row-to-row transfer matrix Equation 3.16 corresponds to adding a row to the lattice, the corner transfer matrix adds a quadrant of spins. It was originally defined by Baxter as

$$A_{\sigma, \sigma'} = \begin{cases} \sum \prod_{\langle i, j, k, l \rangle} W(\sigma_i, \sigma_j, \sigma_k, \sigma_l) & \text{if } \sigma_1 = \sigma'_1 \\ 0 & \text{if } \sigma_1 \neq \sigma'_1. \end{cases} \quad (3.34)$$

Here, the product runs over groups of four spins that share the same face, and the sum is over all spins in the interior of the quadrant.

In a symmetric and isotropic model such as the Ising model, we have

$$W(a, b, c, d) = W(b, a, d, c) = W(c, a, d, b) = W(d, c, b, a) \quad (3.35)$$

and the partition of an  $N \times N$  lattice is expressed as

$$Z_{N \times N} = \text{Tr } A^4. \quad (3.36)$$

In the thermodynamic limit, this partition function is equal to the partition function of an  $N \times \infty$  lattice, given by Equation 3.17.

The matrix in Equation 3.31, containing the Boltzmann weights of spins along a cut down the middle of an  $N \times \infty$  system, is *approximated* by

$$\rho = A^4. \quad (3.37)$$

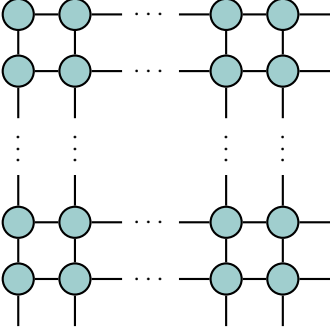


Figure 3.10: Corner transfer matrix expressed as a contraction of  $a$ -tensors.

The difference is that  $\mathcal{A}^4$  represents a square system of size  $N \times N$  with a cut, instead of an  $N \times \infty$  strip with a cut. In the thermodynamic limit, both systems become the same. In the corner transfer matrix renormalization group method,  $\mathcal{A}^4$  is used to find the optimal projector onto  $m$  basis states.

### 3.6.2 Corner transfer matrix as a tensor network

Similarly to how we redefined the row-to-row transfer matrix (Equation 3.16) as the tensor network in Figure 3.5, we can redefine the corner transfer matrix (Equation 3.34) as the tensor network in Figure 3.10. Again, the new and old definitions of  $\mathcal{A}$  are related by a basis transformation

$$\mathcal{A}_{\text{new}} = P \mathcal{A}_{\text{old}} P^T. \quad (3.38)$$

Something about  $\mathcal{A}$  being symmetric. What about non-symmetric cases?

### 3.6.3 Corner transfer matrix renormalization group method

Say something about boundary conditions, also with TMRG algorithm.



The algorithm proceeds very much like the transfer matrix renormalization group method. In addition to renormalizing the half-row transfer matrix  $P$ , we also renormalize the corner transfer matrix  $A$  at each step, using the projector obtained from diagonalizing  $A^4$ .

Compare complexities of both algorithms.

We first initialize  $P_N$  and  $A_N$ , imposing boundary conditions as we see fit.

We then obtain the unrenormalized  $A_{N+1}$  by adding a layer of spins to the quadrant represented by  $A_N$ . This is done by contracting with two half-row transfer matrices  $P_N$  and a single  $a$ -tensor, as shown in the first step of Figure 3.11. We obtain the unnormalized  $P_{N+1}$  as before, as shown in the first step of Figure 3.7.

To find the optimal projector from  $2m$  to  $m$  basis states, we can directly diagonalize  $A_{N+1}^4$ , or, equivalently,  $A_{N+1}$ . As always, we keep the basis states corresponding to the  $m$  largest eigenvectors. This is shown in Figure 3.12. We use the projector to obtain the renormalized versions of  $A_{N+1}$  and  $T_{N+1}$

$$\tilde{A}_{N+1} = O A_{N+1} O^\dagger, \quad (3.39)$$

$$\tilde{T}_{N+1} = O T_{N+1} O^\dagger. \quad (3.40)$$

shown in the second steps of Figure 3.11 and Figure 3.7.

We repeat the above procedure to successively obtain

$$A_{N+1} \rightarrow A_{N+2} \rightarrow \dots, \quad (3.41)$$

$$T_{N+1} \rightarrow T_{N+2} \rightarrow \dots \quad (3.42)$$

until a convergence criterion is reached.

Talk about convergence criterion.

### 3.7 Calculation of observable quantities

To do

### 3.8 Validity of approximation

To do. Talk about spectrum of reduced density matrix/ctm and how it relates to energy gap/correlation length and critical behaviour.

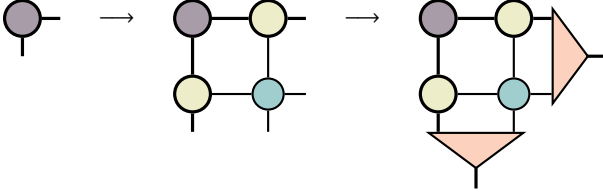


Figure 3.11: In the first step, the unrenormalized  $\mathcal{A}_{N+1}$  is obtained by contracting with two copies of  $P_N$  and a single  $a$ -tensor. This corresponds to adding a layer of spins to the quadrant, thus enlarging it from  $N \times N$  to  $N + 1 \times N + 1$ . In the second step,  $\mathcal{A}_{N+1}$  is renormalized with the projector obtained from diagonalizing  $\mathcal{A}_{N+1}^4$  and keeping the basis states corresponding to the  $m$  largest eigenvalues.

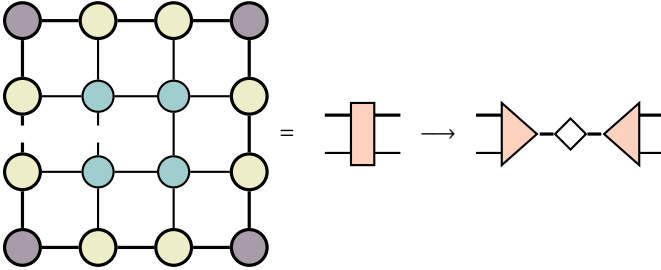


Figure 3.12: The matrix  $\mathcal{A}_{N+1}^4$  is approximately equal to  $\rho_{N+1}$  in Equation 3.31. Compare the graphical forms of this network and the one shown in Figure 3.9. We obtain the optimal projector by diagonalizing  $\mathcal{A}_{N+1}^4$ , or equivalently  $\mathcal{A}_{N+1}$ .

### 3.9 Equivalence to variational approximation in the space of matrix product states.

Talk about Baxter, Rommer and Ostlund, and more recent MPS algorithms. Maybe in appendix?

# 4

## Critical behaviour and finite-size scaling

---

### 4.1 Introduction

Excellent reviews [1], [5].

# A

## Correspondence of quantum and classical lattice systems

---

The partition of a discrete quantum mechanical system is given by

$$Z_q = \text{Tr} \exp(-\beta H_q) = \sum_{\sigma} \langle \sigma | \exp(-\beta H_q) | \sigma \rangle \quad (\text{A.1})$$

Imagine splitting the imaginary time interval  $\beta$  into  $N$  smaller steps:

$$\beta = N \delta \tau, \quad (\text{A.2})$$

$$\exp(-\beta H_q) = \exp(-\delta \tau H_q)^N. \quad (\text{A.3})$$

Recall that for any orthonormal basis, the identity can be expressed as a sum over projectors onto the basis states

$$\mathbb{1} = \sum_{\sigma} |\sigma\rangle \langle \sigma|. \quad (\text{A.4})$$

If we insert  $N - 1$  resolutions of identity into Equation A.1, we obtain

$$Z_q = \sum_{\sigma} \sum_{\sigma_1, \dots, \sigma_{N-1}} \langle \sigma | \exp(-\beta \delta \tau) | \sigma_1 \rangle \dots \langle \sigma_{N-1} | \exp(-\beta \delta \tau) | \sigma \rangle. \quad (\text{A.5})$$

This is the imaginary time path integral formulation of quantum mechanics. Similar to the real-time path integral, an evolution in the imaginary time direction is expressed as a sum over all paths connecting the initial and final state, which are the same here, since we are taking the trace.

We turn to the partition function of a classical system, written as a product of its transfer matrix, as in Equation 3.7:

$$Z_{\text{cl}} = \text{Tr} T^N. \quad (\text{A.6})$$

There is a striking similarity between a quantum mechanical partition function in  $d$  dimensions and a classical partition function in  $d + 1$  dimensions. Adding a row to the classical lattice by applying the transfer matrix corresponds to time evolution of a quantum system:

$$T \longleftrightarrow \exp(-\delta\tau H_q). \quad (\text{A.7})$$

The classical temperature corresponds to the coupling constants in the Hamiltonian  $H_q$ .

Letting  $\beta \rightarrow \infty$  (or equivalently  $T \rightarrow 0$ ) amounts to taking  $N \rightarrow \infty$ , while keeping  $\delta\tau$  fixed. In this limit, analogously to the transfer matrix for the classical system (cf. Equation 3.12), the operator  $\exp(-\beta H_q)$  becomes a projector onto the ground state.

Thus, a quantum lattice in the ground state corresponds to a classical lattice that is infinite in its additional dimension.

What is the role  $\delta\tau$ ? Why should it be small? If we want to make the correspondence  $T \equiv H_q$ , we need  $\delta\tau \rightarrow 0$ . But what does this imply for the lattice? How does the 'scaling limit' come into play? Also: explain the correspondence between the energy scale of the quantum system and the correlation length of the classical system. Maybe do an example of 0D quantum to 1D classical and 1D quantum to 2D classical (Ising model?).

# B

## Introduction to tensor networks

---

### B.1 Tensors, or multidimensional arrays

Make clear that there is a difference between tensors that are defined with a metric.

In the field of tensor networks, a tensor is a multidimensional table with numbers – a convenient way to organize information. It is the generalization of a vector

$$v_i = \begin{bmatrix} v_1 \\ \vdots \\ v_n \end{bmatrix}, \quad (\text{B.1})$$

which has one index, and a matrix

$$M_{ij} = \begin{bmatrix} M_{11} & \dots & M_{1n} \\ \vdots & & \vdots \\ M_{m1} & \dots & M_{mn} \end{bmatrix}, \quad (\text{B.2})$$

which has two. A tensor of rank  $N$  has  $N$  indices:<sup>1</sup>

$$T_{i_1 \dots i_N}. \quad (\text{B.3})$$

A tensor of rank zero is just a scalar.

---

<sup>1</sup>The definition of rank in this context is not to be confused with the rank of a matrix, which is the number of linearly independent columns. Synonyms of tensor rank are tensor degree and tensor order.

## B.2 Tensor contraction

Tensor contraction is the higher-dimensional generalization of the dot product

$$\mathbf{a} \cdot \mathbf{b} = \sum_i a_i b_i, \quad (\text{B.4})$$

where a lower-dimensional tensor (in this case, a scalar, which is a zero-dimensional tensor) is obtained by summing over all values of a repeated index.

Examples are matrix-vector multiplication

$$(\mathbf{M}\mathbf{a})_i = \sum_j M_{ij} a_j, \quad (\text{B.5})$$

and matrix-matrix multiplication

$$(\mathbf{A}\mathbf{B})_{ij} = \sum_k A_{ik} B_{kj}, \quad (\text{B.6})$$

but a more elaborate tensor multiplication could look like

$$w_{abc} = \sum_{d,e,f} T_{abcdef} v_{def}. \quad (\text{B.7})$$

As with the dot product between vectors, matrix-vector multiplication and matrix-matrix multiplication, a contraction between tensors is only defined if the dimensions of the indices match.

## B.3 Tensor networks

A tensor network is specified by a set of tensors, together with a set of contractions to be performed. For example:

$$M_{ab} = \sum_{i,j,k} A_{ai} B_{ij} C_{jk} D_{kb}, \quad (\text{B.8})$$

which corresponds to the matrix product  $ABCD$ .



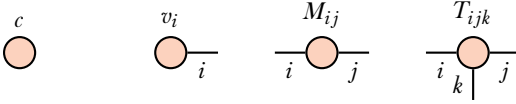


Figure B.1: Open-ended lines, called legs, represent unsummed indices. A tensor with no open legs is a scalar.

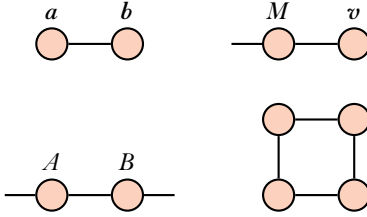


Figure B.2: Connected legs represent contracted indices. The networks in the figure represent  $\sum_i a_i b_i$  (dot product),  $\sum_j M_{ij} a_j$  (matrix-vector product),  $\sum_k A_{ik} B_{kj}$  (matrix-matrix product) and  $\text{Tr } ABCD$ , respectively.

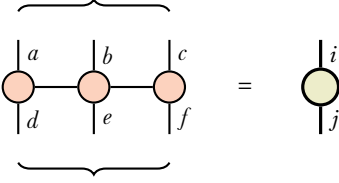
### B.3.1 Graphical notation

It is highly convenient to introduce a graphical notation that is common in the tensor network community. It greatly simplifies expressions and makes certain properties manifest.

Each tensor is represented by a shape. Open-ended lines, called legs, represent unsummed indices. See Figure B.1. If it is clear from the context, index labels may be omitted from the open legs.

Each contracted index is represented by a connected line. See Figure B.2.

Many tensor equations, while burdensome when written out, are readily understood in this graphical way. As an example, consider the matrix trace in Figure B.2, where its cyclic property is manifest.

Figure B.3: Reshaping a tensor  $T_{abcdef}$  to  $T_{ij}$ 

### B.3.2 Reshaping tensors

Several indices can be taken together to form a single, joint index, that runs over all combinations of the indices that fused into it. For example, an  $m \times n$  matrix can be reshaped into an  $mn$  vector.

$$M_{ij} = v_a \quad a \in \{1, \dots, mn\}. \quad (\text{B.9})$$

Some convention has to be chosen to map the joint index  $i, j$  onto the single index  $a$ , for example

$$a = (n - 1)i + j, \quad (\text{B.10})$$

which orders the indices of the matrix  $M$  row by row

$$11, 12, \dots, 1n, 21, 22, \dots, mn - 1, mn. \quad (\text{B.11})$$

Graphically, an index contraction is represented as a bundling of the open legs of a tensor network. See Figure B.3 for an example.

### B.3.3 Computational complexity of contraction

Computational complexity.

## Bibliography

---

- [1] M. N. Barber. “Finite-size Scaling”. In: *Phase Transitions and Critical Phenomena*. Ed. by Cyril Domb and J. L. Lebowitz. Vol. 8. Academic press, 1983. Chap. 2.
- [2] RJ Baxter. “Dimers on a rectangular lattice”. In: *Journal of Mathematical Physics* 9.4 (1968), pp. 650–654.
- [3] RJ Baxter. “Variational approximations for square lattice models in statistical mechanics”. In: *Journal of Statistical Physics* 19.5 (1978), pp. 461–478.
- [4] Rodney J Baxter. *Exactly solved models in statistical mechanics*. Elsevier, 1982. Chap. 13.
- [5] John Cardy. *Scaling and renormalization in statistical physics*. Vol. 5. Cambridge university press, 1996.
- [6] Ernst Ising. “Beitrag zur theorie des ferromagnetismus”. In: *Zeitschrift für Physik* 31.1 (1925), pp. 253–258.
- [7] Richard B Lehoucq and Danny C Sorensen. “Deflation techniques for an implicitly restarted Arnoldi iteration”. In: *SIAM Journal on Matrix Analysis and Applications* 17.4 (1996), pp. 789–821.
- [8] Tomotoshi Nishino. “Density matrix renormalization group method for 2D classical models”. In: *Journal of the Physical Society of Japan* 64.10 (1995), pp. 3598–3601.
- [9] Tomotoshi Nishino and Kouichi Okunishi. “Corner transfer matrix renormalization group method”. In: *Journal of the Physical Society of Japan* 65.4 (1996), pp. 891–894.
- [10] Reinhard M Noack and Steven R White. “The Density Matrix Renormalization Group”. In: *Density-matrix renormalization, a new numerical method in physics*. Ed. by Ingo Peschel et al. Vol. 528. 1999. Chap. 2.

- [11] David Poulin et al. “Quantum simulation of time-dependent Hamiltonians and the convenient illusion of Hilbert space”. In: *Physical review letters* 106.17 (2011), p. 170501.
- [12] Ulrich Schollwöck. “The density-matrix renormalization group”. In: *Reviews of modern physics* 77.1 (2005), pp. 263–265.
- [13] Steven R White. “Density matrix formulation for quantum renormalization groups”. In: *Physical Review Letters* 69.19 (1992), p. 2863.
- [14] Steven R White. “Density-matrix algorithms for quantum renormalization groups”. In: *Physical Review B* 48.14 (1993), p. 10345.
- [15] Steven R White and RM Noack. “Real-space quantum renormalization groups”. In: *Physical review letters* 68.24 (1992), p. 3487.
- [16] Kenneth G Wilson. “The renormalization group: Critical phenomena and the Kondo problem”. In: *Reviews of Modern Physics* 47.4 (1975), p. 773.